JOURNAL OF CATALYSIS 98, 540–549 (1986)

Catalytic Oxidation of Methane on Polycrystalline Palladium Supported on Stabilized Zirconia

SAVVAS SEIMANIDES AND MICHAEL STOUKIDES

Chemical Engineering Department, Tufts University, Medford, Massachusetts 02155

Received July 29, 1985; revised October 29, 1985

The oxidation of methane on porous polycrystalline palladium supported on yttria-stabilized zirconia was studied at atmospheric total pressure in a continuous-stirred tank reactor (CSTR) at temperatures between 450 and 600°C. The technique of solid-electrolyte potentiometry (SEP) was used to measure *in situ* the thermodynamic activity of oxygen adsorbed on the catalyst surface. The reaction kinetics are consistent with an Eley–Rideal model according to which adsorbed atomic oxygen reacts with gaseous methane. The potentiometric measurements suggest that only one oxygen atom is involved in the rate-limiting step. A kinetic model that satisfies both kinetic and SEP results is discussed. © 1986 Academic Press, Inc.

INTRODUCTION

The oxidation of methane has been receiving increased attention in recent years due to its potential industrial interest. Methane is known for its abundance and its chemical stability. When oxidized it produces mainly carbon dioxide and water. Methanol and formaldehyde have been reported to be the most important intermediate products of both the homogeneous and the heterogeneous oxidation of methane (*1*–*3*). Selectivities to such products are very low (*4*, *5*). Nevertheless, since direct formation of formaldehyde and/or methanol from methane would offer a viable alternative to the usual industrial routes (*4*), various workers have investigated the nature and role of intermediate products of the catalytic oxidation of methane in an effort to isolate appreciable quantities of such compounds (*6*–*15*). Recently Liu *et al.* were able to isolate formaldehyde and methanol during the partial oxidation of methane over a silica-supported molybdena catalyst (*16*, *17*). Their observations were confirmed by Khan and Somorjai who further expanded their kinetic studies by measuring the pressure and temperature dependence of the individual rates of formation of methanol and formaldehyde (*18*).

Palladium catalysts have been reported to give best results concerning selectivities to oxygenated products (*6*, *8*, *9*, *12*). Firth studied the kinetics of methane oxidation on Pd–Au alloys as well as the effect of methane on methanol oxidation (*10*). Cullis *et al.* studied the oxidation of CH_4 on Pd catalysts and the effect of halogen compounds on the yield and the selectivity to formaldehyde (*8*). Mann and Dosi examined the above reaction over Pd-supported on Al_2O_3 (*12*). Both groups of investigators report a substantial increase of the selectivity to formaldehyde when halogen modifiers are introduced in the reactor although the yield decreases to some extent (*8*, *12*). Cullis and Willat also studied the kinetics of methane oxidation over palladium and platinum catalysts supported on a number of metal oxides (*19*). Despite the number of investigators who have studied the Pd-catalyzed methane oxidation the reaction mechanism remains unknown.

It has been recently found that the oxidation of methane on porous polycrystalline Ag films supported on yttria-stabilized zirconia is most probably of an Eley–Rideal type of adsorption-reaction with adsorbed atomic oxygen reacting with gaseous methane (*20*). A detailed kinetic study of the Pd-catalyzed oxidation of methane is the sub-

0021-9517/86 $3.00

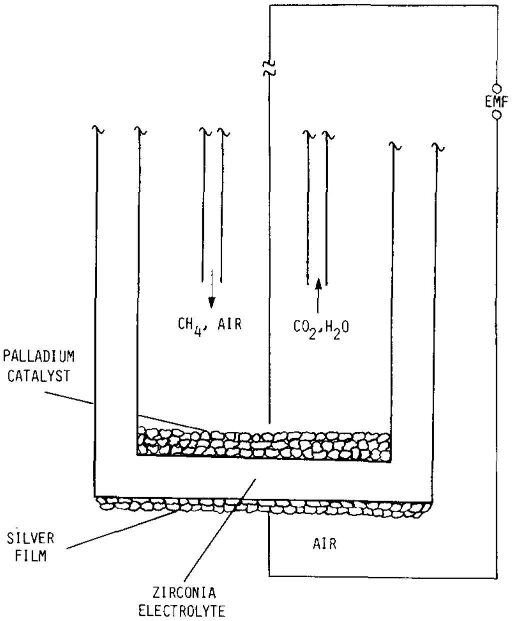

FIG. 1. Schematic diagram of the reactor cell.

ject of the present communication. Kinetics are combined with *in situ* electrochemical measurement of the activity of oxygen adsorbed on the catalyst surface using the technique of solid-electrolyte potentiometry. The technique has already been used in conjunction with kinetic measurements in order to study the mechanism of various catalytic oxidations (*20–22*). Reactor cells similar to the one used in this study have been used so far (a) as electrochemical oxygen "pumps" (*23–25*) and (b) as high-temperature solid electrolyte fuel cells (*26–28*).

The present study is the first stage of an attempt to increase the selectivity to oxygenated products during methane oxidation by using the technique of electrochemical oxygen "pumping." This technique has been used to increase the yield and the selectivity to ethylene oxide during ethylene oxidation (*25*).

EXPERIMENTAL METHODS

The experimental apparatus used for the kinetic and potentiometric studies has been described in detail elsewhere (*20*). A schematic diagram of the reactor cell used is shown in Fig. 1. The palladium catalyst film was deposited on the flat bottom of an 8% yttria-stabilized zirconia tube using an A-2985 palladium resinate solution obtained from Engelhard Corporation. A few drops of the palladium resinate solution were deposited on the flat bottom of the tube followed by drying at 100°C for 4 h. The catalyst was calcined at 550°C for 6 h and heated further to 650°C for 4 h. A silver film was deposited on the outside wall of the zirconia tube. A silver emulsion in butyl acetate obtained from G. C. Electronics was used for that purpose. This film was exposed to air and served as the reference electrode. Silver instead of palladium was used as reference electrode mainly because silver adheres to the zirconia wall much stronger than palladium. This caused a slight (3–5 mV) change in the reference measurements and was appropriately taken into account in the oxygen activity calculations.

The continuous-flow reactor used has been previously described and shown to be well mixed over the range of flow rates employed in the present study (*20*).

The open-circuit emf of the oxygen concentration cell was measured with a Fluke 8600A millivoltmeter. The correct performance of the oxygen concentration cell was verified by introducing into the reactor various air–N_2 mixtures of known P_{O_2} and obtaining agreement within 1–2 mV with the Nernst equation

$$E = \frac{RT}{2F} \ln \left(\frac{P_{O_2}}{0.21}\right)^{1/2}. \qquad (1)$$

The reactants were AIRCO certified CH_4 diluted in N_2 and zero grade air. They could be further diluted in N_2. Calibrated flowmeters were used to measure the total flow rate. A dual-column Perkin–Elmer Sigma 3B gas chromatograph with a T.C. detector was used to analyze on-line reactants and products. A Porapak Q column separated CO_2, H_2O, and air and a molecular sieve 5A column separated N_2, O_2, CH_4 at room tem-

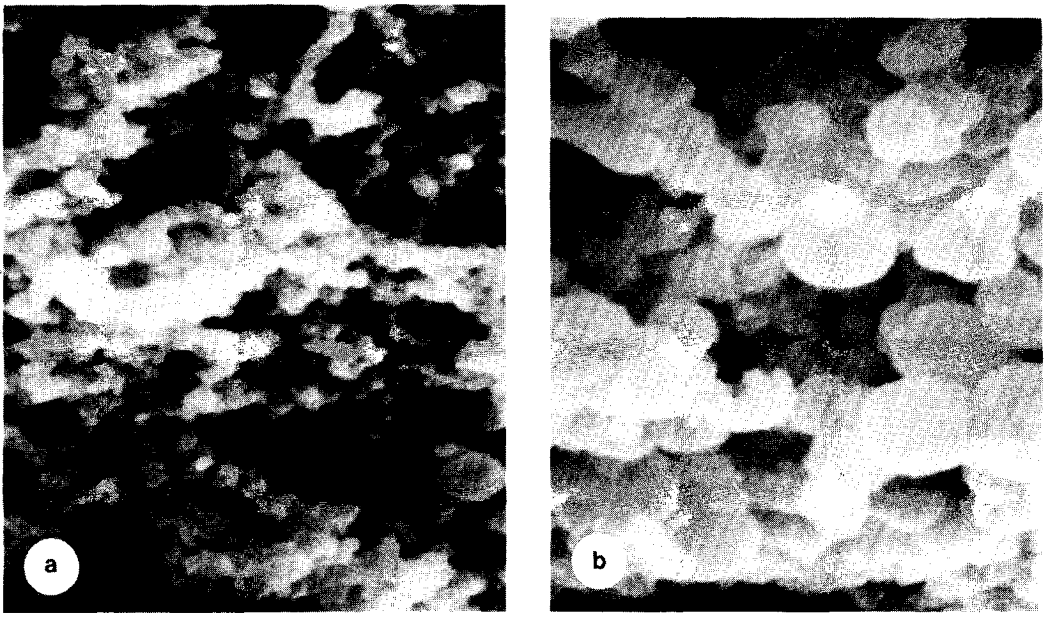

FIG. 2. Scanning electron micrograph of the palladium catalyst (a) before and (b) after reaction (×6000).

perature. The concentration of CO_2 in the effluent stream was also monitored by means of an Infrared Industries Model 703D Infrared CO_2 analyzer. At steady state the CO_2 concentration as measured by the IR analyzer was in very good agreement (within 3%) with the GC measurement.

Typical scanning electron micrographs of the palladium catalyst-electrode before and after reaction are shown in Figs. 2a and b, respectively. The average diameter of the palladium crystallites after reaction was approximately 1–1.5 μm. The catalyst loading used in these experiments was 190 mg of Pd and using the above crystallite size a total catalyst surface area of 370–390 cm^2 was estimated.

MEASUREMENT OF THE OXYGEN ACTIVITY

The technique of solid electrolyte potentiometry (SEP) was used to measure *in situ* the thermodynamic activity of oxygen on the Pd catalyst. Originally proposed by Wagner (*29*) SEP has been used so far in a number of kinetic studies. The open-circuit emf of the solid-electrolyte cell reflects the difference in chemical potential of oxygen adsorbed on the two electrodes (*29*):

$$E = \frac{1}{4F} [\mu_{O_2}\,(\text{catalyst}) - \mu_{O_2}\,(\text{reference})], \quad (2)$$

where F is the Faraday constant and E the measured open-circuit emf.

The chemical potential of oxygen adsorbed on the reference electrode which is in contact with air ($P_{O_2} \simeq 0.21$ bar) is given by

$$\mu_{O_2}\,(\text{reference}) = \mu^{\circ}_{O_2}\,(\text{g}) + RT\ln(0.21), \quad (3)$$

where $\mu^{\circ}_{O_2}$ (g) is the standard chemical potential of oxygen at the temperature of interest. Similarly the activity a_0 of adsorbed oxygen on the catalyst surface can be defined as

$$\mu_{O_2}\,(\text{catalyst}) = \mu^{\circ}_{O_2}\,(\text{g}) + RT\ln a_0^2. \quad (4)$$

Therefore, a_0^2 expresses the partial pressure of gaseous oxygen that would be in equilibrium with oxygen adsorbed on the catalyst surface, if such an equilibrium were established. Combining Eqs. (2), (3), and (4)

$$a_0 = (0.21)^{1/2} \exp\left(\frac{2FE}{RT}\right). \quad (5)$$

Equation (5) permits direct calculation of the surface oxygen activity by simply measuring the temperature and the open-circuit emf of the cell. Under conditions of thermodynamic equilibrium between surface and gaseous oxygen:

$$a_0 = P_{O_2}^{1/2}$$

Equation (2) reduces in this case to the usual Nernst equation (Eq. (1)) used to verify the correct performance of the cell.

RESULTS

Kinetic Measurements

The kinetics were studied at temperatures between 450 and 600°C, methane partial pressures between 1.23×10^{-2} and 7.85×10^{-2} bar and oxygen partial pressures between 0.24×10^{-2} and 6.83×10^{-2} bar. The total pressure of the mixture was 1 bar. Nitrogen was used as a diluent. P_{CH_4} or P_{O_2} could be maintained at a desired level by varying the partial pressure of nitrogen.

Homogeneous gas phase oxidation of methane was insignificant over the temperature range where the heterogeneous reaction was investigated (*20*).

After an initial induction period which lasted approximately 48 h the catalyst activity remained constant within 3% for at least 8 weeks. All the data reported below were obtained after the termination of the induction period.

The absence of external diffusional effects was verified by varying the total flowrate at constant gas composition and observing negligible change on the reaction rate. The absence of internal diffusion limitations was verified by varying the film thickness of the porous Pd catalyst and observing no change (<2%) in the surface oxygen activity for the same temperature and gas composition. This proves the absence of diffusional effects inside the catalyst pores since the oxygen activity is measured at the gas–metal–zirconia interline and is a function of gas composition (*20–22*).

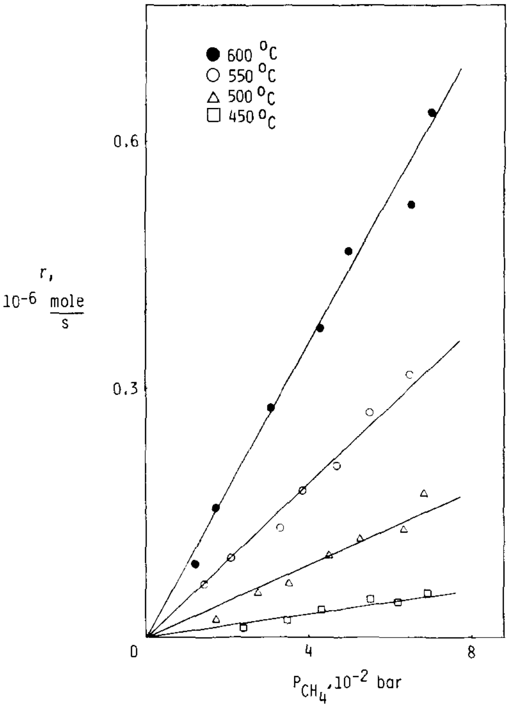

FIG. 3. Dependence of reaction rate on methane partial pressure.

In all the range of temperatures and gas compositions examined, only CO_2 and H_2O were observed as products at measurable quantities.

The reaction rate r (molecules of methane consumed/s) was calculated from the raw kinetic data of the CSTR using the appropriate mass balance:

$$r = GX_{CO_2}, \quad (6)$$

where X_{CO_2} is the mole fraction of CO_2 in the effluent stream and G is the total molar flow rate.

Table 1 contains kinetic and potentiometric results of this study.

The rate of CO_2 formation is plotted in Fig. 3 vs the partial pressure of methane in the reactor at constant T and P_{O_2}. The rate

TABLE I

Kinetic and Potentiometric Data

T (°C)	P_{CH_4} (10^{-2} bar)	P_{O_2} (10^{-2} bar)	a_0	r (10^{-6} mol/s)	T (°C)	P_{CH_4} (10^{-2} bar)	P_{O_2} (10^{-2} bar)	a_0	r (10^{-6} mol/s)
600	7.22	0.25	0.043	0.345	500	6.53	0.35	0.051	0.086
	7.82	0.31	0.049	0.345		6.71	0.62	0.069	0.103
	7.63	0.52	0.065	0.398		6.97	0.78	0.078	0.104
	7.35	0.84	0.083	0.480		6.76	2.46	0.130	0.114
	7.58	1.46	0.110	0.527		7.41	3.24	0.158	0.134
	7.51	2.32	0.139	0.555		7.25	4.67	0.185	0.142
	7.58	4.15	0.191	0.589		7.47	5.96	0.210	0.142
	7.85	5.62	0.228	0.614		7.63	1.12	0.094	0.123
	1.23	6.70	0.264	0.088		1.46	6.40	0.253	0.219
	1.72	6.83	0.261	0.155		2.76	6.70	0.252	0.054
	3.08	6.40	0.254	0.276		3.52	6.52	0.230	0.065
	4.33	6.35	0.248	0.374		4.49	6.35	0.230	0.098
	5.00	6.14	0.238	0.467		5.25	6.40	0.225	0.120
	6.55	5.66	0.226	0.523		6.33	6.31	0.225	0.129
	7.03	5.88	0.228	0.636		6.82	6.57	0.220	0.174
550	7.00	0.24	0.042	0.149	450	6.99	0.50	0.057	0.040
	6.89	0.39	0.056	0.180		7.30	0.82	0.075	0.044
	6.90	0.62	0.069	0.187		7.62	1.08	0.080	0.046
	7.09	0.99	0.081	0.226		7.85	2.40	0.128	0.050
	7.25	1.73	0.118	0.264		7.63	3.80	0.160	0.050
	7.14	3.00	0.165	0.307		7.79	4.67	0.180	0.063
	7.20	4.80	0.216	0.342		7.45	0.33	0.046	0.039
	7.14	6.48	0.254	0.334		2.39	6.74	0.244	0.011
	1.41	6.74	0.263	0.063		3.46	6.40	0.226	0.022
	2.11	7.13	0.261	0.095		4.33	6.18	0.209	0.032
	3.30	6.57	0.252	0.132		5.52	6.18	0.216	0.044
	3.84	6.70	0.247	0.177		6.17	5.83	0.205	0.043
	4.71	6.70	0.245	0.206		6.93	6.05	0.205	0.055
	5.47	6.74	0.244	0.272					
	6.49	6.77	0.243	0.318					

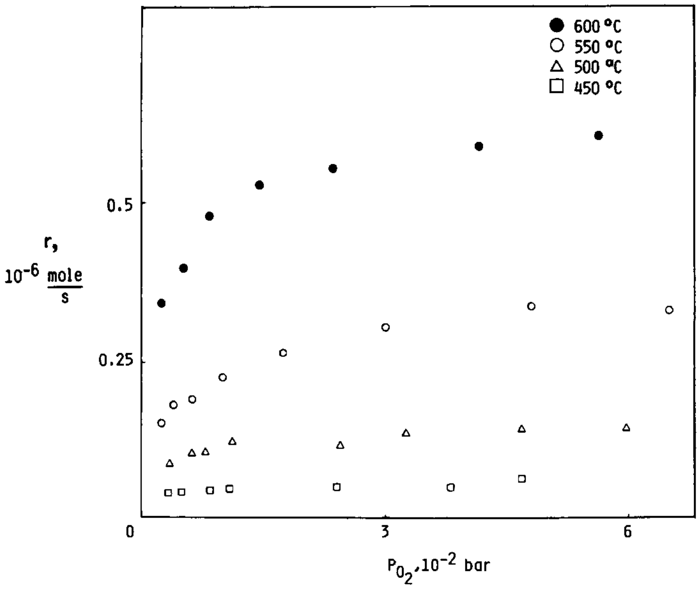

FIG. 4. Dependence of reaction rate on oxygen partial pressure.

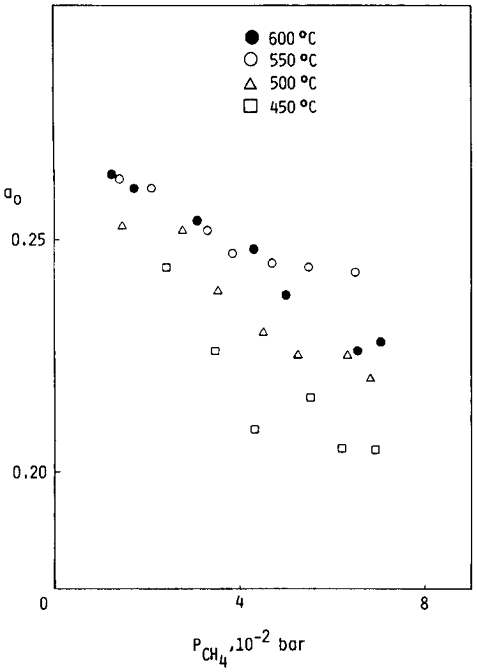

FIG. 5. Dependence of surface oxygen activity on methane partial pressure.

is linearly proportional to methane partial pressure. The dependence of the reaction rate on P_{O_2} for constant P_{CH_4} is shown in Fig. 4. At low oxygen partial pressures the rate tends to be proportional to P_{O_2} while at high P_{O_2} it becomes almost independent of P_{O_2}.

Oxygen Activity Measurements

It was observed that in general, during methane oxidation on Pd, $a_0 \simeq P_{O_2}^{1/2}$. This was also the case during the study of the methane oxidation over silver (*20*). On the contrary, during the hydrogen oxidation on nickel catalyst $a_0 \ll P_{O_2}^{1/2}$ (*22*). This difference is justified by the relatively lower rates obtained during CH₄ oxidation over both Pd and Ag.

The dependence of the surface oxygen activity on the partial pressure of methane for constant P_{O_2} is shown in Fig. 5 for 450, 500, 550, and 600°C. Fig. 6 is a plot of a_0 vs P_{O_2}. Figures 5 and 6 indicate that (a) a_0 increases with increasing P_{O_2} (b) a_0 decreases weakly with increasing P_{CH_4}, (c) a_0 is almost independent of temperature for constant P_{O_2} and P_{CH_4}.

It was found that all the measurements could be correlated rather accurately by the equations

$$\left(\frac{P_{O_2}}{a_0^2} - 1\right)\frac{1}{P_{CH_4}} = K_1 + K_2 a_0^{-1} \tag{7}$$

with

$$K_1 = 2.92 \times 10^{-4} \exp\left(\frac{7000}{T}\right) \tag{8}$$

and

$$K_2 = 0.501 \exp\left(-\frac{1300}{T}\right). \tag{9}$$

This is shown in Fig. 8. The relation between the reaction rate and the surface oxygen activity was found to satisfy the equation

$$\frac{P_{CH_4}}{r} = K_3 + K_4 a_0^{-1} \tag{10}$$

with

$$K_4 = 195 \exp\left(\frac{3600}{T}\right) \tag{11}$$

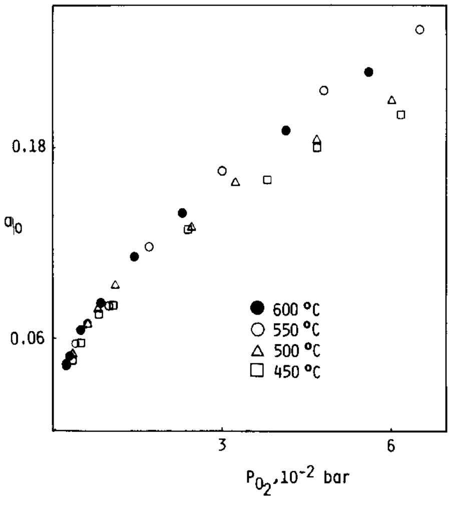

FIG. 6. Dependence of surface oxygen activity on oxygen partial pressure.

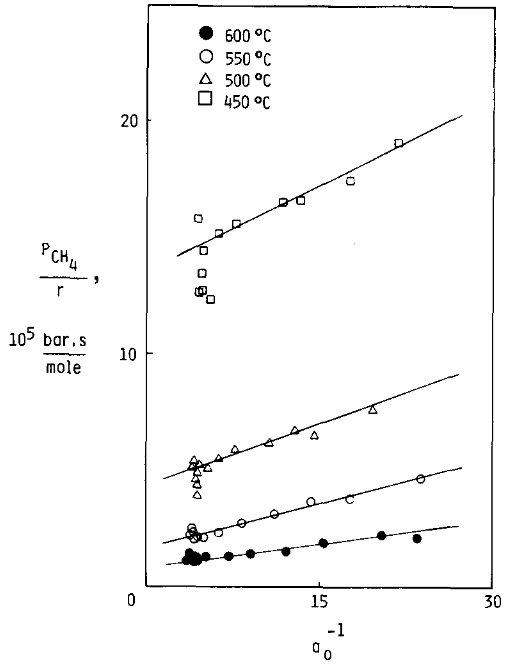

FIG. 7. Dependence of reaction rate on a_0.

and

$$K_3 = 0.114 \exp\left(\frac{11{,}900}{T}\right). \quad (12)$$

This is shown in Fig. 7 for 450–600°C. The scattering in the data shown in Figs. 7 and 8 and especially at low values of a_0^{-1} is mainly due to the fact previously mentioned, i.e., that $P_{O_2} \simeq a_0^2$ and thus the difference $(P_{O_2}/a_0^2 - 1)$ takes very low values and is very sensitive to experimental error.

DISCUSSION

Little information is available on the mechanism of methane oxidation on palladium. Firth suggested that methane is probably adsorbed on top and reacts with a layer of oxygen which is strongly bound to the catalyst surface (*10*). Cullis *et al.* suggested that methyl or methylene radicals react with surface lattice oxygen (*8*) and their observations were further supported by the work of Yu YaO (*13*). Mann and Dosi (*12*) proposed a kinetic model according to which charged adsorbed methane reacts with charged adsorbed oxygen. We will attempt to present below a kinetic model that takes into account both kinetic and potentiometric results obtained in this study.

Oxygen is known to adsorb dissociatively on palladium (*30, 31*). Furthermore in the temperature range within which the heterogeneous oxidation of methane is usually studied (300–700°C) formation of palladium oxide is thermodynamically fa-

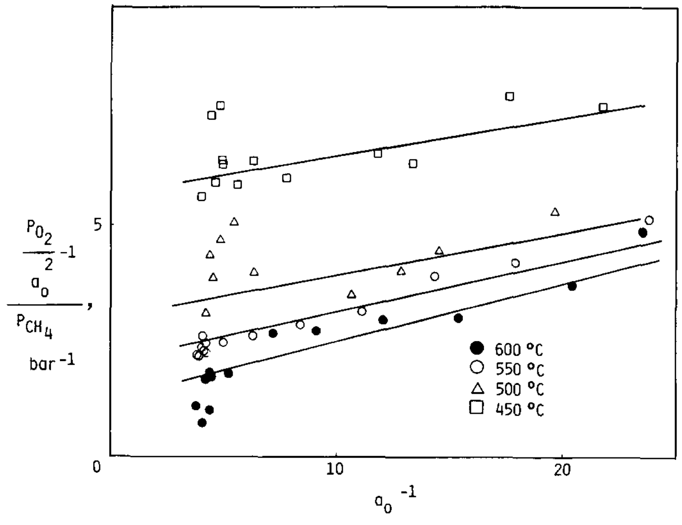

FIG. 8. Dependence of a_0 on gas-phase composition.

vored (*19, 32, 33*). Campbell *et al.* (*33*) found significant oxygen uptake for oxygen partial pressures smaller than the equilibrium (dissociation) pressure of PdO. The above authors concluded that a solid solution of low concentration of oxygen in Pd was formed and that this solution was probably a precursor to the formation of bulk stoichiometric oxide (*33*). Guiot suggested that the oxidation of palladium proceeds to the formation of a three-dimensional surface compound before the formation of PdO (*34*). Turner and Maple studied recently (*31*) the rate of PdO formation at temperatures of 160–640°C and atmospheric pressure. According to their work two distinct types of oxygen reside on the surface, chemisorbed oxygen and a more strongly bound oxide species. Chemisorbed oxygen adsorbs only at the surface and in order for oxide species to be formed oxygen must be first chemisorbed (*31*). Presence of PdO during CH_4 oxidation has been reported by Cullis and Willat who examined Pd catalysts by XPS (*19*).

It is therefore reasonable to consider that in the present study the Pd surface may be largely oxidized to PdO. If more than one type of oxygen reside on the catalyst surface the property a_0 measured by SEP reflects their common activity provided that these species are in thermodynamic equilibrium. In the opposite case, i.e., when the various oxygen species are not in equilibrium, a_0 reflects the activity of those species that will equilibrate faster with O^{2-} at the three phase zirconia–catalyst–air interline (*22, 29*). In the present study the less strongly bound to the surface atomic oxygen is the species the activity of which is measured electrochemically. Consequently following the definition (*20*) of a_0 one can write

$$\theta_0 = \frac{K_0 a_0}{1 + K_0 a_0}, \qquad (13)$$

where K_0 is the adsorption coefficient and θ_0 is the coverage of atomically chemisorbed oxygen. The above equation relating two intrinsic surface properties is valid irrespective of whether equilibrium between gas phase and adsorbed oxygen exists or not.

The rate of CH_4 oxidation to CO_2 and H_2O shown in Table 1 and in Figs. 3 and 4 can be compared to the rate of PdO formation as measured by Turner and Maple (*31*). If palladium oxide reacts with CH_4 then at steady state a material balance for oxygen of the oxide gives

$$R_{\text{PdO}} = 4r,$$

where R_{PdO} is the rate of PdO formation and r is the rate of CH_4 oxidation. (The coefficient 4 accounts for the four atoms of O required to oxidize completely one molecule of methane.) In the temperature range 450–600°C R_{PdO} is calculated to be at least two orders of magnitude lower than the rate of methane oxidation. At lower temperatures, e.g., 200–350°C the two rates may become comparable because of the different activation energies of the two reactions (~20 kcal/mol for CH_4 oxidation and ~5 kcal/mol for PdO formation). Therefore the interpretation that we can provide is that the less strongly bound oxygen species oxidize methane to CO_2 and H_2O. Hence palladium oxide either (a) is not reduced by methane and thus the catalyst consists largely of palladium oxide or (b) reacts with methane before steady state is established in which case all the oxide originally present on the catalyst is consumed. Note that all our measurements were obtained at steady state and at least 15–20 min after the introduction of the reacting mixture in the reactor.

Based on the available data it is not possible to discriminate among the above alternative schemes.

Figure 4 shows that the rate of reaction is independent of the partial pressure of oxygen with the exception of 550 and 600°C where at low P_{O_2}/P_{CH_4} the rate becomes almost proportional to P_{O_2}. Figure 3 shows that the rate is first order in P_{CH_4} at all temperatures and gas compositions examined.

Based on the above observations we can propose an Eley–Rideal type of adsorption-reaction according to which gaseous methane reacts with adsorbed atomic oxygen. Assuming that one oxygen atom is involved in the rate-limiting step the rate of CH_4 oxidation will be given by

$$r = K_R P_{CH_4} \theta_0. \tag{14}$$

Substituting for θ_0 from Eq. (13) one gets

$$r = K_R P_{CH_4} \frac{K_0 a_0}{1 + K_0 a_0}. \tag{15}$$

Taking the reciprocals of both terms of Eq. (15) and multiplying both by P_{CH_4} it follows that

$$\frac{P_{CH_4}}{r} = \frac{1}{K_R} + \frac{1}{K_R K_0} \frac{1}{a_0} \tag{16}$$

which reduces to the experimentally derived Eq. (10) for $K_3 = 1/K_R$ and $K_4 = 1/K_R K_0$. Consequently,

$$K_R = 8.81 \exp\left(-\frac{11{,}900}{T}\right) \frac{\text{mol}}{\text{s} \cdot \text{bar}} \tag{17}$$

and from the values of K_4 (slopes of the lines in Fig. 7) one can calculate

$$K_0 = 5.82 \times 10^{-4} \exp\left(\frac{8300}{T}\right). \tag{18}$$

Since K_0 is the adsorption coefficient of atomic oxygen it follows from Eq. (18) that $\Delta H_0 = -16.5$ kcal/g-atom O and $\Delta S_0 = -14.8$ cal/g-atom O where ΔH_0 and ΔS_0 are the enthalpy and entropy of adsorption of atomic oxygen, respectively.

The surface oxygen activity dependence on temperature and gas composition can be explained by considering a steady-state mass balance for adsorbed oxygen:

$$K_A P_{O_2}(1 - \theta_0)^2 = K_D \theta_0^2 + 2\, K_R P_{CH_4} \theta_0. \tag{19}$$

The left-hand side term corresponds to atomic oxygen adsorption which is assumed to be dissociative. The right-hand side terms correspond to desorption and reaction with gaseous methane. Assuming that PdO is formed via chemisorbed oxygen as it has been previously suggested (*31*) one more term should be added to the right-hand side of equation (19), i.e., the rate of palladium oxide formation from chemisorbed oxygen. However, we can neglect that term as being much smaller than the rate of methane oxidation in the temperature range of our interest. Dividing Eq. (19) by $K_A(1 - \theta_0)^2$ one obtains

$$P_{O_2} = \frac{K_D}{K_A} \frac{\theta_0^2}{(1 - \theta_0)^2} + 2 \frac{K_R}{K_A} \frac{\theta_0}{(1 - \theta_0)^2} P_{CH_4}. \tag{20}$$

Taking into account Eq. (13) and that $K_0^2 = K_A/K_D$ Eq. (20) becomes

$$P_{O_2} = a_0^2 + 2 \frac{K_R}{K_D K_0} a_0(1 + K_0 a_0) P_{CH_4}$$

or

$$\frac{P_{O_2}}{a_0^2} = 1 + 2 \frac{K_R}{K_D K_0} \left(K_0 + \frac{1}{a_0}\right) P_{CH_4}. \tag{21}$$

When $P_{CH_4} \rightarrow 0$ equilibrium is established between gaseous and adsorbed oxygen, i.e., $P_{O_2} = a_0^2$. Therefore, Eq. (21) can be rearranged to give

$$\frac{P_{O_2}}{a_0^2} - 1 = 2 \frac{K_R}{K_D} P_{CH_4} + 2 \frac{K_R}{K_D K_0} P_{CH_4} \frac{1}{a_0} \tag{22}$$

which reduces to the experimentally observed Eq. (7) for

$$K_1 = 2K_R/K_D$$

and

$$K_2 = 2K_R/K_D K_0.$$

Having obtained K_0 and K_R we can extract the value for K_D. It is thus found that

$$K_D = 6.04 \times 10^4 \exp\left(\frac{-18{,}900}{T}\right) \frac{\text{mol } O_2}{\text{s}} \tag{23}$$

From the values of K_0 and K_D given by Eqs. (18) and (23), respectively, we can further calculate the adsorption rate constant for atomic oxygen:

$$K_{\mathrm{A}} = K_0^2 \cdot K_{\mathrm{D}} = 2.05 \times 10^{-2} \exp\left(\frac{-2300}{T}\right) \frac{\text{mol } \mathrm{O}_2}{\text{s}}. \tag{24}$$

The above presented model explains both kinetic and potentiometric results in a satisfactory manner. Note that although not unique the above model was the one among a large number of models examined that satisfied most successfully our experimental results.

In summary it has been shown that when SEP is used in conjunction with kinetic measurements it can provide substantial information for the mechanism of catalytic oxidations on metal surfaces. It is well established that kinetic information is insufficient for determining the mechanism of a reaction. Much more information is necessary to establish a mechanism of a catalytic reaction. Use of other *in situ* spectroscopic techniques such as infrared spectroscopy could further elucidate the mechanism of these important catalytic systems.

ACKNOWLEDGMENT

We gratefully acknowledge the National Science Foundation for support of this work through NSF Grant CPE 8507317.

REFERENCES

1. Margolis, L. Y., "Advances in Catalysis," Vol. 14, p. 429. Academic Press, New York, 1963.
2. Dixon, J. K., and Longfield, J. E., *in* "Catalysis" (P. H. Emmett, Ed.), Vol. 7. Reinhold, New York 1960.
3. Walker, J. F., "Formaldehyde," 3rd ed. Reinhold, New York, 1967.
4. Kirk-Othmer, "Encyclopedia of Chemical Technology," 3rd. ed. Wiley, New York, 1978.
5. Satterfield, C. N., "Heterogeneous Catalysis in Practice." McGraw–Hill, New York, 1980.
6. Schonfelder, R., *Ber. Ges. Kohlentech.*, 247 (1923).
7. Berl, K., and Fischer, B., *Z. Angew. Chem.* **36,** 297 (1923).
8. Cullis, C. F., Keene, D. E., and Trim, D. L., *J. Catal.* **19,** 378 (1970).
9. Reyerson, L. H., and Swearingen, L. E., *J. Phys. Chem.* **31,** 88 (1927).
10. Firth, J. G., *Trans. Faraday Soc.* **62,** 2566 (1966).
11. Firth, J. G., and Holland, H. B., *Nature (London)*, **217,** 1252 (1968).
12. Mann, R. S., and Dosi, M. K., *J. Chem. Technol. Biotechnol.* **29,** 467 (1979).
13. Yung-Fang Yu Yao, *Ind. Eng. Chem. Process. Res. Dev.* **19,** 293 (1980).
14. Anderson, R. B., Stein, K. C., Feenan, J. J., and Hofner, L. J. E., *Ind. Eng. Chem.* **53,** No. 10, 809 (1961).
15. Mezaki, R., and Watson, C. C., *Ind. Eng. Chem. Process. Des. Dev.* **5,** 62 (1966).
16. Liu, R. S., Iwamoto, M., and Lunsford, J. H., *J. Chem. Soc. Chem. Commun.* **1,** 78 (1982).
17. Liu, H. F., Liu, R. S., Liew, K. Y., Johnson, R. E., and Lunsford, J. H., *J. Amer. Chem. Soc.* **106,** 4117 (1984).
18. Khan, M. M., and Somorjai, G. A., *J. Catal.* **91,** 263 (1985).
19. Cullis, C. F., and Willatt, B. M., *J. Catal.* **83,** 267 (1983).
20. Seimanides, S., and Stoukides, M., *J. Catal.* **88,** 490 (1984).
21. Vayenas, C. G., Lee, B., and Michaels, J., *J. Catal.* **66,** 36 (1980).
22. Saranteas, C., and Stoukides, M., *J. Catal.* **93,** 417 (1985).
23. Pancharatnam, S., Huggins, R. A., and Mason, D., *J. Electrochem. Soc.* **122,** 869 (1975).
24. Gür, T. M., and Huggins, R. A., *Solid State Ionics* **5,** 563 (1981).
25. Stoukides, M., and Vayenas, C. G., *J. Catal.* **70,** 137 (1981).
26. Etsell, T. H., and Flengas, S. N., *J. Electrochem. Soc.* **118,** 12, (1971).
27. Vayenas, C. G., and Farr, R. D., *Science (Washington)* **208,** 593 (1980).
28. Farr, R. D., and Vayenas, C. G., *J. Electrochem. Soc.* **127,** 7 (1980).
29. Wagner, C., "Advances in Catalysis," Vol. 21, p. 323. Academic Press, New York, 1970.
30. Conrad, H., Ertl, G., Kuppers, J., and Latta, E. E., *Surf. Sci.* **65,** 245 (1977).
31. Turner, J. E., and Maple, M. B., *Surf. Sci.* **147,** 647 (1984).
32. Mallika, C., Sreedharan, O. M., and Gnanamoorthy J. B., *J. Less-Common Met.* **95,** 213 (1983).
33. Campbell, C. T., Foyt, D. C., and White, J. M., *J. Phys. Chem.* **81,** 491 (1977).
34. Guiot, J. M., *J. Appl. Phys.* **39**(7), 3509 (1968).